Tellus (1996), 48B, 197–212
Printed in Belgium – all rights reserved

TELLUS
ISSN 0280–6509

Aerosol number size distributions from 3 to 500 nm diameter in the arctic marine boundary layer during summer and autumn

By DAVID S. COVERT*, *Dept. of Atmospheric Sciences, University of Washington, Seattle WA 98 195, USA*, ALFRED WIEDENSOHLER**, *Dept. of Nuclear Physics, Lund University, S-223 62 Lund, Sweden*, PASI AALTO, *Dept. of Physics, University of Helsinki, SF-00170, Helsinki, Finland*, JOST HEINTZENBERG**, *Dept. of Meteorology, Stockholm University, S-106 91 Stockholm, Sweden*, PETER H. MCMURRY, *Dept. of Mechanical Engineering, University of Minnesota, Minneapolis, MN 55455, USA* and CAROLINE LECK, *Dept. of Meteorology, Stockholm University, S-106 91 Stockholm, Sweden*

(Manuscript received 6 April 1994; in final form 29 June 1995)

ABSTRACT

Aerosol physics measurements made onboard the Swedish icebreaker *Oden* in the late Summer and early Autumn of 1991 during the International Arctic Ocean Expedition (IAOE-91) have provided the first data on the size distribution of particles in the Arctic marine boundary layer (MBL) that cover both the number and mass modes of the size range from 3 to 500 nm diameter. These measurements were made in conjunction with atmospheric gas and condensed phase chemistry measurements in an effort to understand a part of the ocean-atmosphere sulfur cycle. Analysis of the particle physics data showed that there were three distinct number modes in the submicrometric aerosol in the Arctic MBL. These modes had geometric mean diameters of around 170 nm, 45 nm and 14 nm referred to as accumulation, Aitken and ultrafine modes, respectively. There were clear minima in number concentrations between the modes that appeared at 20 to 30 nm and at 80 to 100 nm. The total number concentration was most frequently between 30 and 60 particles cm^{-3} with a mean value of around 100 particles cm^{-3}, but the hourly average concentration varied over two to three orders of magnitude during the 70 days of the expedition. On average, the highest concentration was in the accumulation mode that contained about 45% of the total number, while the Aitken mode contained about 40%. The greatest variability was in the ultrafine mode concentration which is indicative of active, nearby sources (nucleation from the gas phase) and sinks; the Aitken and accumulation mode concentrations were much less variable. The ultrafine mode was observed about two thirds of the time and was dominant 10% of the time. A detailed description and statistical analysis of the modal aerosol parameters is presented here.

1. Introduction

Aerosols in the Arctic are recognized to be of importance to atmospheric chemistry and climate. Numerous studies have documented both the chemistry and physics in several locations including Arctic Haze events in the late Winter and much cleaner conditions in the Summer (Lannefors et al., 1983; Rahn, 1981; Davidson and Schnell, 1993; Heintzenberg and Leck, 1994). In the Summer of 1991 the International Arctic Oceanic Expedition was undertaken onboard the Swedish icebreaker *Oden* and an extensive aerosol physics experiment was included to extend previous aerosol observations to the inner Arctic as a part of a study of the natural sulfur cycle.

The natural sulfur cycle in the troposphere

* Corresponding author.
** Presently at, Institute for Tropospheric Research, Permoserstr. 15, D-04303 Leipzig, Germany.

involves release of dimethylsulfide (DMS) from the ocean surface that is oxidized photochemically or by heterogeneous reactions in the atmosphere and eventually converted in part to sulfate compounds in the particulate phase. Regional and global models of the atmosphere which couple chemistry and radiative transfer have demonstrated that aerosols in anthropogenically perturbed areas have a climate forcing effect due to their direct interaction with solar radiation. This forcing could be comparable in magnitude but opposite in sign to the forcing expected of greenhouse gases (Charlson et al., 1991, 1992; Penner et al., 1992). The model results are still quantitatively uncertain without further experimental validation of the input and output data but the uncertainty is not great enough that this aerosol effect can be considered negligible. There is also a further indirect effect of aerosols on radiative transfer through the action of the aerosol as cloud condensation nuclei (CCN) and modification of cloud albedo (Twomey, 1977) and cloud stability (Albrecht, 1989). These effects have not been quantified but qualitative relationships have been observed on the global and local scales (Durkee et al., 1991; Radke et al., 1989). The physical and chemical characteristics of the aerosol in the remote regions of the atmosphere, unperturbed by anthropogenic sources, are important input conditions for such models on scales from the microphysical to global.

The International Arctic Ocean Expedition in 1991 (IAOE-91) was a joint effort that enabled research in the remote, central Arctic ocean basin within the atmospheric, oceanographic and geological sciences. Measurements within the atmospheric program were taken aboard the icebreaker *Oden* during 13 separate time periods (atmospheric chemistry stations) and at times in-between when it was possible to combine atmospheric sampling with other programs onboard. The cruise was conducted between August 1 and October 8, 1991. About 6 days were spent between latitude 70° N and 80° N, 22 days between 80° N and 85° N, and 27 days north of 85° N. Altogether this enabled sampling in open water, the marginal ice zone and in the pack ice. A map and further description of the cruise are presented by Leck et al. (1996).

Detailed measurements of the physical and chemical properties of aerosol in the Arctic marine boundary layer (MBL) was an integral part of the experiment. The goal of the aerosol physics measurements reported here was to measure and analyze in detail the number size distribution of the aerosol over the range 3 nm to 500 nm. This wide range encompasses the number modes and mass mode of the submicrometric aerosol and in particular those subsets of the particle population that are related to several atmospheric chemistry processes and atmospheric effects. Particle formation and transformation may occur in-situ in the Arctic MBL or aerosol may be transported to the Arctic at the surface or in the free troposphere and mixed to the surface from aloft. The absolute concentration and distribution of particles over the range 3 to 500 nm reflects the source, formation processes and age of the aerosol. Although the sea salt particles larger than 500 nm may be involved in the sulfur cycle as a sink for sulfur dioxide (SO_2), methane sulfonic acid (MSA) and sulfuric acid (H_2SO_4), these particles were not studied physically.

Quantification of the concentration and size distribution of "ultrafine" particles, the subset from 3 to 25 nm that has been predicted to occur in undisturbed marine environment (Junge, 1972), was of particular interest in this experiment. This was done first to compare and evaluate instrumental methods for detecting these particles and second to determine their concentration as a measure of the strength and variability of particle nucleation in or near the Arctic MBL as a source of new particles. It was hypothesized that especially under Arctic conditions of low accumulation mode number concentration and low aerosol surface area coupled with low temperature, high relative humidity (RH) and DMS concentration, and near continuous daylight, sulfuric acid vapor production would at times lead to new particle formation by binary (or higher order) homogeneous nucleation of $H_2SO_4 \cdot nH_2O$. There is a potentially large variability in the particle formation rate due to its highly non-linear dependence on these parameters (Peters and Easter, 1994). Under some conditions the formation rate may be high and the concentration of newly formed particles may be many thousands per cubic cm while under slightly different conditions the formation rate and concentration may be orders of magnitude lower. Due to their relatively short lifetime, the presence of ultrafine particles, especially at the lower limit of

our measurement range, is an indication of recent production.

Once formed, these ultrafine particles grow by coagulation and vapor deposition to sizes in the "Aitken" range from 25 to 80 nm. Under conditions in the remote troposphere growth out of the ultrafine range is likely to be relatively fast, on the order of hours, while subsequent growth through the Aitken range takes days (Raes et al., 1993). Further growth can occur via heterogeneous processes in non-precipitating cloud droplets since particles at the upper end of this Aitken range are active CCN at the water vapor supersaturations in cumulus and stratocumulus clouds (Hoppel et al., 1994a, b). This cloud processing transforms particles to a size in the "accumulation" range of 100 to 500 nm. These particles constitute the overwhelming fraction of the mass concentration. They determine the optical properties of the submicrometric aerosol and are active as CCN in stratus and stratocumulus clouds and fog.

In this paper the statistics of the aerosol number size distribution, its modal concentrations, mean diameters and geometric standard deviations are presented along with interpretation of the major features and their time variation in relation to the meteorological conditions. The Arctic aerosol measurements presented here are the first to cover the wide size range and to be so extensive in time and latitude.

2. Experimental approach

2.1. Sampling

For simultaneous sampling of atmospheric aerosol and trace gases, the air was drawn from about 25 m above the sea surface into the laboratory via ducts on a three masted inlet system that extended at an angle of 45° to about 3 m above the roof of the laboratory container. The sampling system for both gases and particles and the experimental methods used for chemical and gas analysis are described in detail in companion papers by Leck and Persson (1996a, b) and Leck et al. (1996). 2 of the 3 masts were used for aerosol sampling for aerosol chemistry and physics. The aerosol physics duct had an impactor (Anderson Samplers, Inc. Atlanta, GA) installed at the inlet to remove particles larger than 10 μm diameter, the aerosol physics instrumentation was connected to a 10 mm diameter sampling tube and distribution manifold.

2.2. Aerosol physics measurements

During the cruise, 5 different instrumental approaches were used to measure the aerosol number size distribution over the diameter range 3 nm to 500 nm. Details of the instruments and their calibration and intercomparison prior to the expedition have been presented by Wiedensohler et al. (1994). These tests showed that the differential mobility particle sizers for the ultrafine (UDMPS) and the Aitken plus accumulation (DMPS) size ranges provided the best measure of the distribution between 8 and 500 nm while an ultrafine condensation particle counter with pulse height analysis (UCPC:PHA) provided the best definition of particle concentration in the range below 5 nm. Two other instruments, a diffusion battery with an ultrafine particle counter and an ultrafine particle counter with a variable saturator-condenser temperature difference were found to give less well defined particle concentration and sizing information in the size range less than 10 nm and the analysis of the data from these instruments is not included here.

A differential mobility analyzer (DMA, Knutson and Whitby, 1975; Liu and Pui, 1974) and an ultrafine differential mobility analyzer (UDMA, Winklmayr et al., 1991) were used to size particles from 20 to 500 nm and 3 to 20 nm, respectively. The sensor for the DMA was a condensation particle counter (CPC, model 3760, TSI Inc., St. Paul, MN, USA); the sensor for the UDMA was an ultrafine condensation particle counter (UCPC, model 3025, TSI). The combination of size definition and sensing constitutes the systems, DMPS and UDMPS mentioned above. Both sensors were calibrated for counting efficiency as a function of size with respect to a monodisperse particle source and an electrometer as an independent particle detector. During the IAOE-91 on the *Oden* the two mobility analyzers were operated in a stepwise scanning mode starting from 20 nm diameter and stepping upwards (or downwards, respectively) in size to produce a distribution measurement every 10 min. Equal logarithmic mobility steps of about 11 channels per decade were used in the scans for a total of 34 diameter intervals, D_i. The data were

inverted from a mobility distribution to a number size distribution assuming a bipolar charge distribution (Wiedensohler, 1988). The UCPC:PHA was calibrated with monodisperse sulfuric acid and ammonium sulfate particles and determined to have a sensitive range of 2.7 to 5 ± 1 nm. While the instrument provides size information within that range, the data were integrated and taken simply as the number concentration for that entire interval. This provides concentration information in that size range which is much more certain than that from the UDMPS due to the low charging efficiency in that range. A separate, independent measure of total particle number concentration greater than 3 nm, $[N_{\text{total}}]$, was made with a UCPC which sampled the aerosol directly for 2 out of every 10 min.

2.3. *Analysis*

The data set encompasses the thirteen atmospheric chemistry stations of the IAOE-91 cruise as well as most of the intervening time during the period from 1 August through 8 October. The data were edited to eliminate periods of possible contamination from the ship and related activities. Time periods when total number concentration was greater than 2000 cm^{-3} were arbitrarily edited as being likely due to contamination. While atmospheric nucleation events or transport from other regions of the troposphere can produce higher concentrations (Clarke, 1993; Covert et al., 1992) we had no independent means of distinguishing these possible events from either direct or aged contamination from the ship. The time variation of $[N_{\text{total}}]$ could be used as an indicator of direct contamination but this variable was not measured with adequate time resolution. Since only a few instances of $[N_{\text{total}}]$ above 2000 cm^{-3} were observed for consecutive measurements (2 min out of 10), analysis of these few instances would have been tenuous even if these high concentrations were from uncontaminated atmospheric conditions. Due to the low particle counting rate in the smaller and larger size channels the data were averaged over periods of an hour to reduce the counting uncertainty (Wiedensohler et al., 1994). Visual analysis of the data showed that the majority of the inverted distributions were bimodal or trimodal with clear separation of the modes.

2.4. *Size distribution parameterization and internal consistency tests*

The size distribution fitting algorithm DistFit™ (Whitby et al., 1991) was used to parameterize the hourly number distribution data from the DMPS and UDMPS according to the best fit to a unimodal, bimodal or trimodal log normal distribution function. The fitting algorithm produced three parameters for each fitted mode, the integral number in the mode, the geometric mean diameter of the mode and its geometric standard deviation. These are symbolized as $[N_m]$, $D_{gn,m}$ and $\sigma_{gn,m}$ where the subscript m refers to the modes, ultrafine, Aitken or accumulation. The bimodal fit was selected in cases when the trimodal fit produced an insignificant or unrealistic mode either with respect to number concentration ($<1\%$ of total and <1 cm^{-3}), overlap of another mode (less than a factor of 1.3 difference in mean size) or a large standard deviation (>3). Similarly, a single mode was selected if one of the remaining modes was unrealistic. A trimodal fit was selected as best 65% of the time; a bimodal fit was selected 25% of the time. This parameterization allowed the size distribution data set to be reduced from 34 concentrations as a function of size to 9 parameters which are more independent than concentrations in the adjacent measured size increments. Furthermore, they can be readily presented, evaluated and used in multivariate analysis and in models. The sum of the modal number concentrations, $[\sum N_m]$, was calculated for comparison to the directly measured $[N_{\text{total}}]$ and the sum of the size distribution, $[\sum N(D_i)]$.

Several tests of the internal consistency of the instrumental and analytical techniques were made. A comparison of the directly measured number concentration $[N_{\text{total}}]$ and the sum of the measured number size distribution $[\sum N(D_i)]$ was made. (The data were edited to include hours when both instruments were operational at least half the time, about 1000 h.) The regression coefficient for this data set was 0.94 and the coefficient of determination, R^2, was 0.90. For the subsets of this data at concentrations of <300 cm^{-3} (shown in Fig. 1) and <10 cm^{-3} the value of the regression coefficient increased to 0.96 and R^2 increased to 0.98 for both cases. The 99.9% confidence intervals for the slope (shown in the plot) deviated less than 3% from the regression line. The reason for the

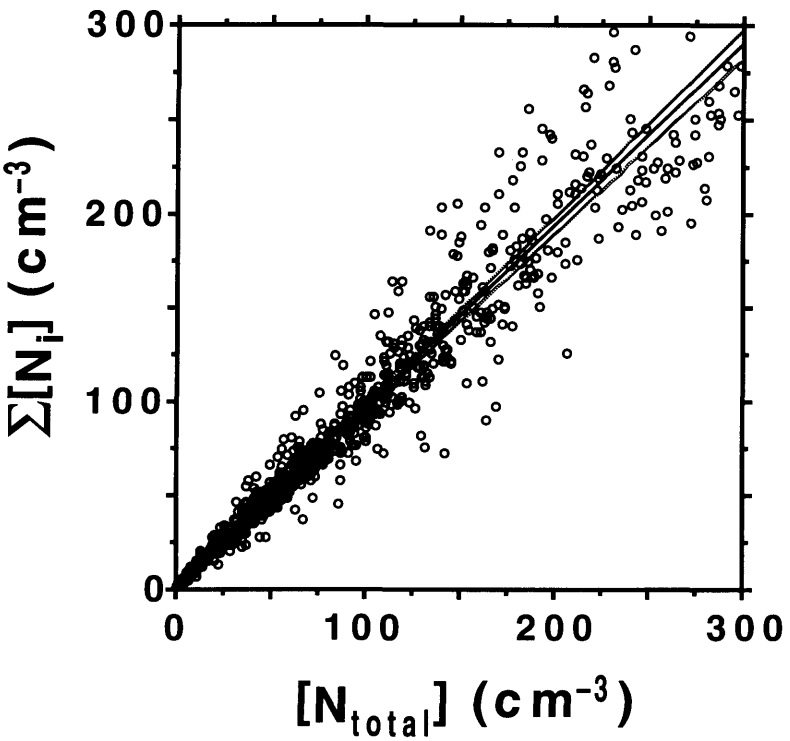

Fig. 1. Correlation between particle number concentration measured directly with the UCPC, $[N_{total}]$, and the integral of the number size distribution measured with the UDMPS and DMPS, $\sum [N_i]$. The calculated regression line with 99.9 % confidence limits for the slope are shown. The regression equation was $\sum [N_i] = 1 + 0.96 \cdot [N_{total}]$.

lower regression coefficient at high concentrations is not clear but was obviously caused by a group of about 40 data points which lie well below the regression line and which constitute a distinct, separate mode in the frequency distribution of the ratio $[\sum N(D_i)]/[N_{total}]$. Without those points the regression coefficient for the data set as a whole was 0.96 as well. Thus, in general the comparison was good and the difference was within our ability to set and maintain equal flow rates in the instruments.

Another test of the consistency of the measurements is the difference in the two size distribution measurements at their point of overlap, 20 nm. Since the UDMPS scanned down in size and the DMPS scanned up in size from this point there is no timing difference to affect the comparison at this size. The UDMPS yielded a concentration at this size that was consistently low by about 10%. Flows were calibrated with the same standard and the same charge distribution was used in the inversion calculations. The discrepancy is likely due to the difference in the operation of the different DMAs.

The DistFit™ results provided a good parameterization of number concentration, mean diameter and standard deviation for the modes of the distribution. χ^2 values averaged less than 0.1. Further tests relating to the analysis of the modes of the number size distribution were made to determine the accuracy of the fitting of the distribution with the DistFit™ routines in terms of reproduction of the number concentrations in the modal size ranges. The three modal number concentrations and the integral number in the corresponding range from the unfitted number distribution data were compared, i.e., $[\Sigma N_i]$ for each range versus $[N_{ultrafine}]$, $[N_{Aitken}]$ and $[N_{accumulation}]$. Again an R^2 value of greater than 0.95 and a regression coefficient of 1 ± 0.05 were obtained in all cases. This

comparison is of course not a rigorous test, since the minimum between the fitted modes was not a fixed value, but it indicates that the fitting procedure produced reasonable numbers and further that a simpler division of total concentrations according to the minima would be an acceptable way of parameterizing model concentrations in this case. Similarly, the modal diameter was a very good representation of the log normally fit geometric mean diameter.

Based on these tests of the internal consistency of the data set that includes redundant measurements we feel that this data and its analytical results provide an accurate representation of the aerosol in the Arctic MBL and portray its general features and deviations related to specific conditions. Means and distributions of the values of the hourly fitted data were determined for the cruise as a whole, the atmospheric chemistry stations, chemical sampling intervals and periods of interest as indicated by other parameters such as air mass changes, air trajectories, fog, radon concentration or ozone concentration (Leck and Persson, 1996b; Bigg et al., 1996; Nilsson, 1996). Time series and statistics of the number size distribution data for the entire cruise and examples are presented here. The relationships between aerosol and other atmospheric parameters during the cruise, the stations and selected events will be discussed in the companion papers that deal with those individual events.

3. Results and discussion

The extensive aerosol physics data set resulting from this experiment is presented mainly in statistical form with a few examples from specific locations and a time series to illustrate typical number size distributions and the scale of variability. The structure of the distribution contains information about aerosol processes such as new particle formation, cloud processing and mixing between the MBL and the free troposphere. Since there are many concurrent and competing processes that affect the size distribution, interpretation of its structure to derive information about individual processes that may have occurred in the past is complicated and must ultimately rely on models in combination with more detailed data, especially profiles in the vertical. Nevertheless, in many cases one process can dominate the number concentration, especially in a particular size range, and direct conclusions can be drawn.

3.1. Particle number size distributions

Over the duration of the expedition more than 1200 hourly average data sets were derived from measurements of total particle number concentration and size distribution from the UCPC, DMPS, UDMPS and UCPC:PHA instruments. Five selected number size distributions are plotted in Fig. 2 as examples of the hourly average data from the UDMPS and DMPS instruments. For comparison to the measured data, the multimodal, log normal fits to the data are presented on the same plots. The first four plots (Fig. 2a–d) illustrate the variety of distributions that were observed and the accuracy of the log normal fit that was made by DistFit™. The first of these, from Station 4, shows an example of a distribution that was dominated by an ultrafine mode between 3 and 8 nm diameter with a concentration of about 250 cm^{-3}; the combined Aitken and accumulation modes had a concentration of less than 25 cm^{-3}. The low concentration in the larger modes is evidence that this distribution was not the result of direct or aged contamination from the ship plume which would have been much broader even if highly diluted. The second plot, (Fig. 2b) from data taken 18 h after the first and just north of Spitsbergen, was dominated by Aitken mode particles with a shoulder into the ultrafine mode which DistFit™ distinguished as a separate mode. (If the separation of any two modes analyzed by DistFit™ was less than calculated for this example a single mode fit was used for that range of data.) The 5-day air mass back-trajectory at the time was from the direction of the Spitsbergen Archipelago and may represent the effect of increased oceanic DMS source in the vicinity of the archipelago. The third plot (Fig. 2c) illustrates an example of widely separated ultrafine and Aitken modes; more often the ultrafine and Aitken modes were less widely separated, e.g., Fig. 2e, as will be seen in the statistical presentations. Fig. 3d illustrates a case in which there was a high concentration of particles in both the Aitken and accumulation modes and an insignificant concentration of particles in the ultrafine mode. The trajectory in this case originated over N. Europe and moved rather directly from the industrialized Kola Peninsula

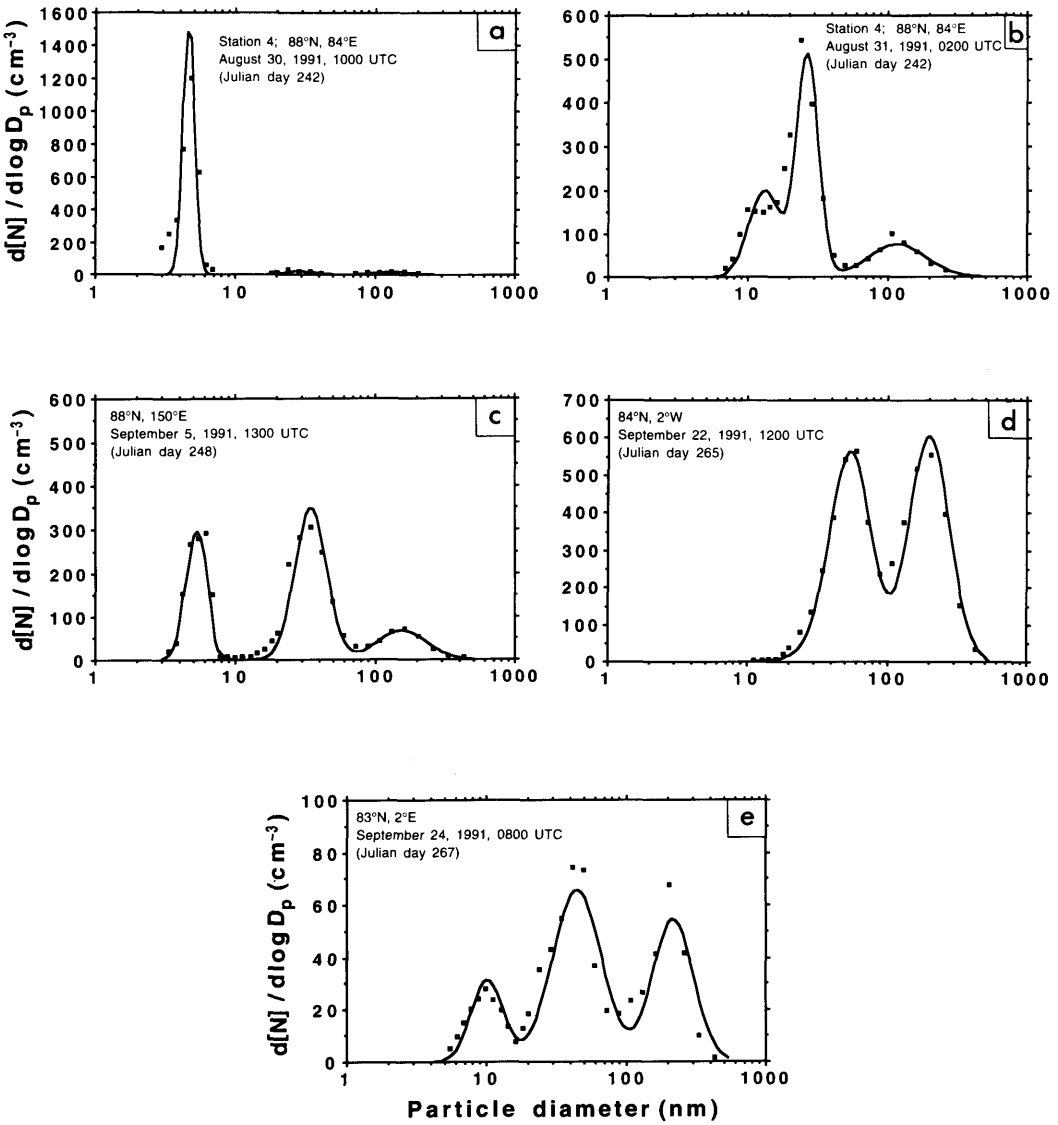

Fig. 2. Particle number size distributions, $d[N]/d \log D_p$; examples of the measured one hour average data and the log normal fits to the modes of the data. Squares are measured data, solid lines are the fitted log normal modes determined by DistFit™. (a) Station 4 (88°N, 84°E), August 30, 1991 at 1000 UTC. As an example of a dominant ultrafine mode. (b) Station 4 (88°N, 84°E), August 31, 1991 at 0200 UTC. Trajectories were from Spitsbergen. Aitken and ultrafine modes are minimally separated. (c) (88°N, 150°E), September 5, 1991 at 1300 UTC. Three widely separated and distinct modes were present. (d) (84°N, 2°W), September 22, 1991 at 1200 UTC. Aerosol concentrations were relatively high and trajectories were from the Kola Peninsula. (e) (83°N, 2°E), September 24, 1991 at 0800 UTC. Typical trimodal distribution from the Arctic MBL.

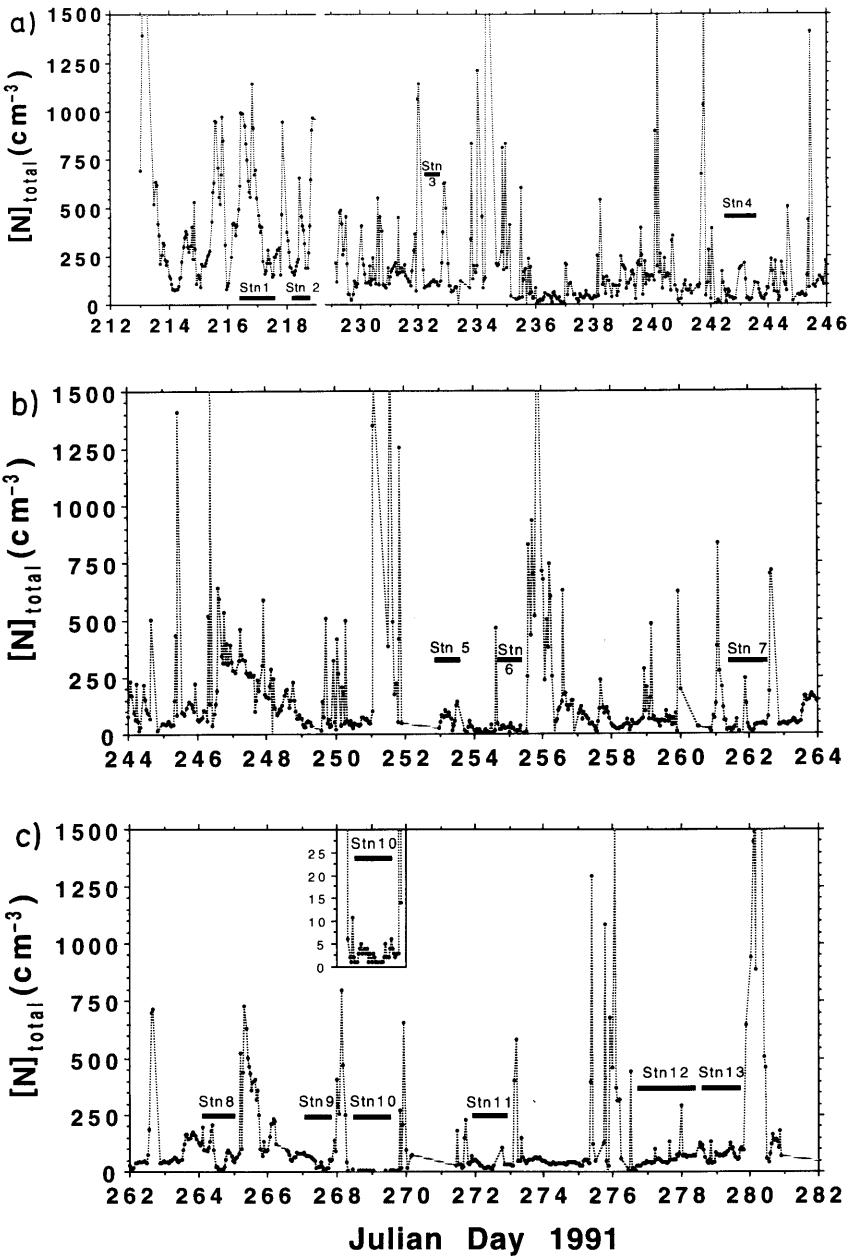

Fig. 3. Time series of total number concentrations [N_{total}] for the duration of the cruise with station times indicated. The inset represents the concentration during station ten with a factor of 50 expansion of the concentration scale to illustrate the low concentrations at that time.

area of the Russian Arctic to the *Oden*. Fig. 2e shows a typical Arctic MBL size distribution with three distinct modes of comparable magnitude. Other examples of size distributions for specific conditions of rapidly changing meteorological conditions or aerosol parameters are presented by Bigg et al. (1996).

These size distributions contrast markedly with those measured over a period of several weeks in late Winter in the Arctic at Ny Ålesund, Spitsbergen, in which the accumulation mode was consistently dominant and the Aitken mode represented about 20% of the total number (Covert and Heintzenberg, 1993). Mean diameters of the accumulation and Aitken modes were larger in the Winter aerosol also. (The ultrafine mode was not measured.)

With respect to the ultrafine and Aitken modes observed in this experiment, similar distributions and stability were observed by Ito (1993) in the Antarctic.

3.2. *Time series data*

A time series of $[N_{\text{total}}]$ for the duration of the cruise is plotted in Fig. 3 along with the station intervals highlighted on the time scale. Clearly, there were many extended periods throughout the cruise when the total number concentration was less than 100 cm^{-3} and stable and thus most likely representative of background Arctic conditions with minimal influence from regional or continental sources of particles. These included most of the stations and several additional periods when the ship was underway. (Similarly, periods of stability were observed in the ultrafine, Aitken and accumulation mode data that are not illustrated here as a time series.) Superimposed on this baseline there were at times large increases in the concentration that were most often due to spikes of one hour or less. At other times concentrations were much lower, notably at station 10 where $[N_{\text{total}}]$ was less than 5 cm^{-3} for a period of 24 h (see expanded inset in Fig. 3).

Some of the high and variable concentrations could be associated with direct transport of air masses from distant sources of pollution, e.g., on days 234 and 265 when trajectories came from Spitsbergen and the Kola peninsula, respectively. However, only 6% of the trajectories originated in areas suspected to be pollution sources. The dominant source of the trajectories was the Arctic MBL (with variable residence times over the pack ice and in the MBL); the second most common source was the free troposphere. Thus, much of the variability in aerosol concentration must be due to sources and processes in the Arctic MBL and the free troposphere above it. Trajectory and air mass chemistry related to variability of aerosol concentrations are presented by Leck and Persson (1996b). These two events of continental influence and other events involving a sudden and marked change in aerosol properties were associated with changes in meteorological and gas phase chemistry parameters and were caused by intermittent, sometimes repeated, mixing in the MBL and are described in detail by Nilsson (1996) and Bigg et al. (1996). Some of the variability at low particle concentration levels was due to the influence of land masses, N. Greenland and Spitsbergen, within the Arctic. Even though there was considerable variability in the particle number concentration for the individual modes and the total there was little variability in the other parameters, geometric mean diameter and geometric standard deviation, D_{gn} and σ_{gn}, respectively. When the data were separated into subsets with total number less than and greater than 250 cm^{-3} there was no significant change in the D_{gn} and σ_{gn} values.

Meteorological and chemical analysis of the situation during Station 10, Julian days 268 and 269, indicated that the extremely low concentrations during this period were due to a change in boundary layer stability and in large scale circulation. Trajectories prior to that time had more direct contact with the biologically productive seas around the ice edge. A change in the synoptic circulation resulted in surface layer trajectories that had longer transport time within the MBL over the pack ice and no direct contact with marine, biological DMS sources in the Arctic. During this time period the stability of the MBL at the *Oden* increased due to strong subsidence at the 900 and 950 mb levels and reduced solar input to the surface. Surface trajectories showed no subsidence. These two conditions prevented the advection of gas phase aerosol precursors from more southerly latitudes in the Arctic and prevented significant mixing of aerosols from aloft. After day 269, subsidence extended all the way to the surface and the aerosol concentrations increased suddenly with input from the free troposphere.

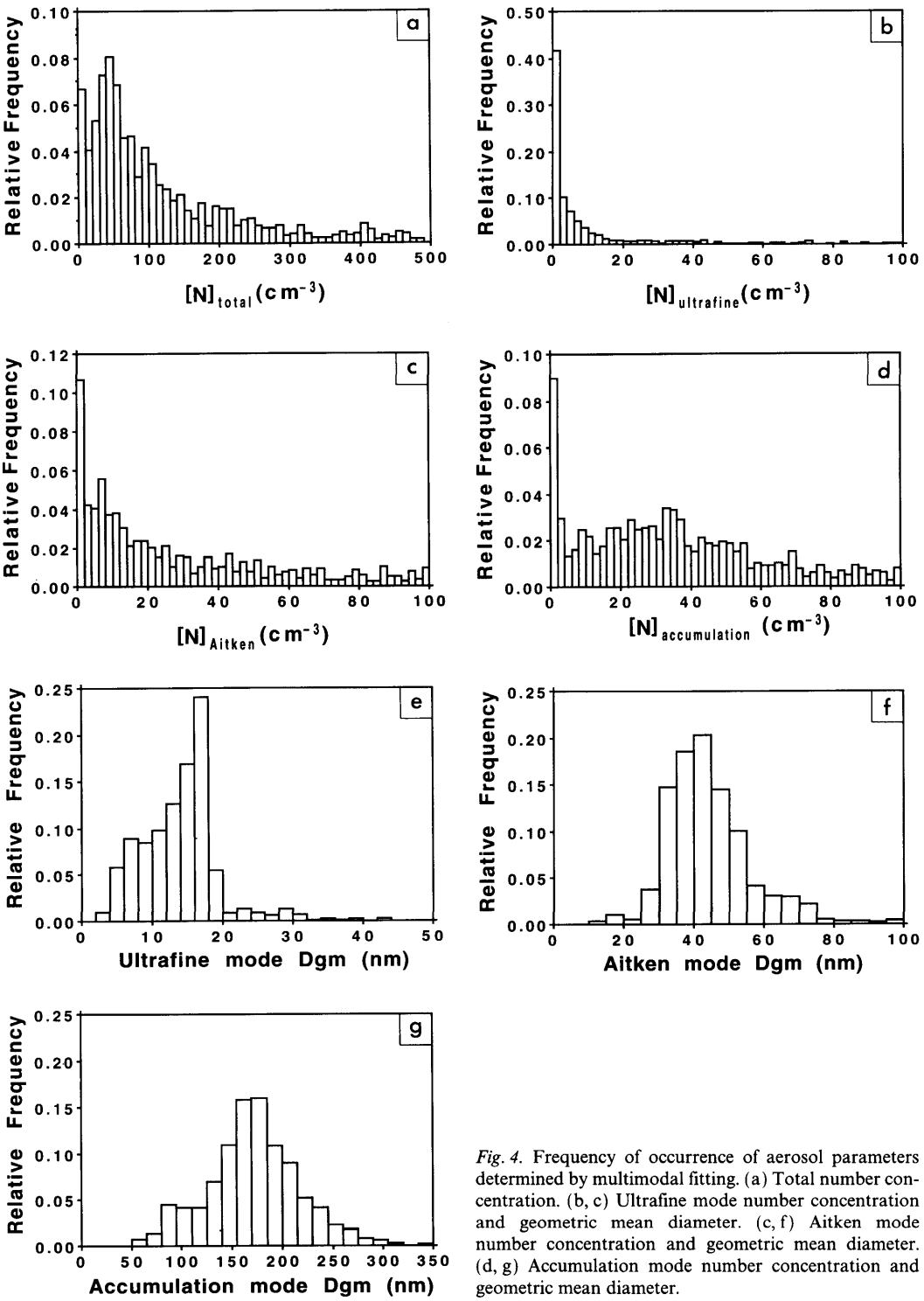

Fig. 4. Frequency of occurrence of aerosol parameters determined by multimodal fitting. (a) Total number concentration. (b, c) Ultrafine mode number concentration and geometric mean diameter. (c, f) Aitken mode number concentration and geometric mean diameter. (d, g) Accumulation mode number concentration and geometric mean diameter.

3.3. *Frequency of occurrence statistics*

Histograms of the relative frequency of occurrence of the modal parameters of concentration and geometric mean diameter for the fitted size distributions are shown in Fig. 4. The geometric standard deviation data for the modes was relatively invariant and is not plotted. The corresponding statistics of all nine parameters of the fitted modes and the total number concentration are presented in Table 1a. The histograms of the number concentration data were all skewed with a tail toward high values which indicates that mean values were not necessarily the most appropriate measures of central tendency of the distributions. Thus, geometric means, median values, inter-quartile ranges and 10% trimmed means, were also calculated for comparison. During times when the ship was on Stations 3 through 13 the total number concentration was lower by about a factor of two on the average and was much less variable. The same result was found for the Aitken and accumulation modes. However, the reduction in concentration and variability was not as great for the ultrafine mode during these times. This result also held true for other times during the cruise

Table 1a. *Descriptive statistics for particulate number size distributions during IAOE-91 from hourly averaged data*

Number concentration

(cm^{-3})	Mean value	Coef. of variation	Geom. mean	Median value	10% trimmed mean	Interquartile range
$[N_{ultrafine}]$	44	3.6	0.6	3	11	18
$[N_{Aitken}]$	90	1.9	14	29	51	84
$[N_{accumulation}]$	60	1.8	18	36	43	52
$[N_{total}]$	194	1.6	81	88	125	167

Geometric mean diameter

(nm)	Mean value	Coef. of variation
$D_{gn\ ultrafine}$	14	0.42
$D_{gn\ Aitken}$	45	0.33
$D_{gn\ accumulation}$	171	0.27

Geometric standard deviation

	Mean value	Coef. of variation
$\sigma_{gn\ ultrafine}$	1.36	0.50
$\sigma_{gn\ Aitken}$	1.50	0.44
$\sigma_{gn\ accumulation}$	1.64	0.25

Table 1b. *Number concentration during periods of low and stable concentrations*

(cm^{-3})	Mean value	Coef. of variation	Geom. mean	Median value	10% trimmed mean	Interquartile range
$[N_{ultrafine}]$	10	2.4	0.2	2	8	4
$[N_{Aitken}]$	34	1.1	7.5	18	44	27
$[N_{accumulation}]$	38	0.8	14	32	37	34
$[N_{total}]$	81	0.8	81	62	82	74

when total number concentrations were less than 250 cm^{-3}. The statistics for this subset of the data at lower concentration are presented in Table 1b. The concentration values for all modes were much more normally distributed for this subset.

As an alternative to summary statistics or grand average presentations of the number size distributions a two dimensional plot of the frequency of occurrence of model number concentrations and modal geometric mean diameters (with contours representing the frequency of occurrence) was generated to give an overview of the entire data set and its range of variability (Fig. 5). It should be noted that this is not a three dimensional presentation of the number distribution itself but rather of the modal parameters. The results of the fitting of the separate ultrafine, Aitken and accumulation modes have been overlaid in this plot to give a composite view of the parameterized concentration and mean diameters of the entire distribution. While there is some overlap of the distribution of geometric mean diameters, the frequency of occurrence for any mode is adequately low in the overlapping ranges 20 to 30 nm and 60 to 110 nm that the composite contour presentation does not distort the result of the marked separation of the modes. The third parameter derived from the fitting routine, geometric standard deviation, had relatively less variability as can be seen from Table 2 and was considered of less importance to the overview picture than concentration and mean size.

There are several features that can be derived from this data. The first is the extreme stability of the mean diameters and standard deviations of the modes of the size distribution, especially the Aitken and accumulation modes, in spite of the order of magnitude variability in particle concentration and varied meteorology and atmospheric chemistry during the cruise. There was relatively

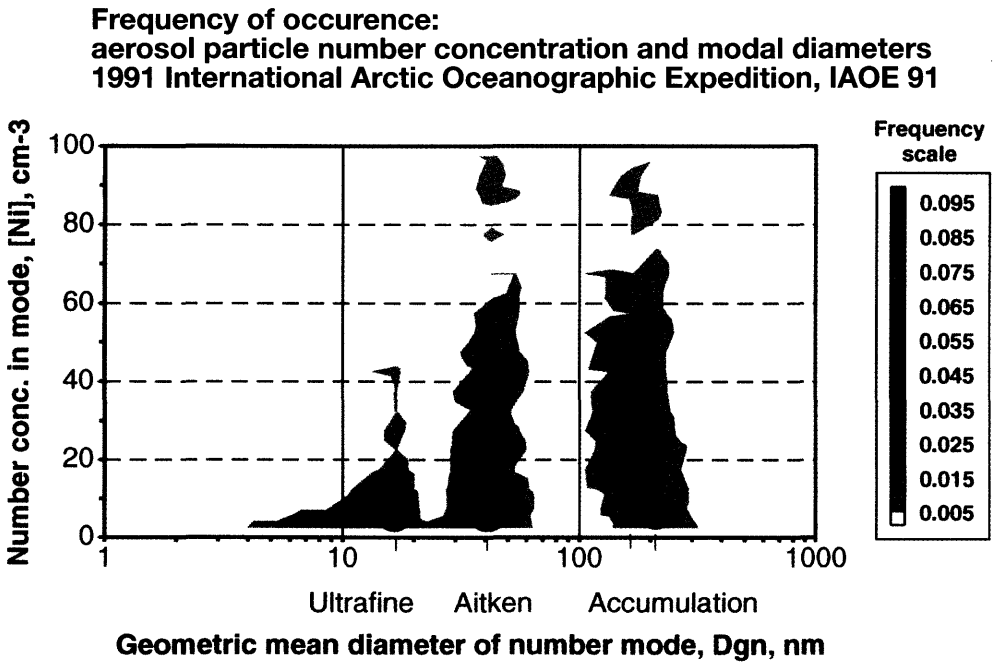

Fig. 5. Composite, two-dimensional frequency of occurrence plot of modal number concentration and geometric mean diameter. For each of the three modes the frequency of occurrence parameter is plotted as the color contour versus modal concentration on the ordinate and diameter on the abscissa. The data represents a total of 1180 hourly observations or 82% of the cruise hours. The ultrafine mode occurred in 755, the Aitken in 1014 and the accumulation in 1085 of the observations.

more variability in the mean diameter of the ultrafine mode and less variability in concentration. Another remarkable feature is the uniform presence and consistency of the minima between the modes.

3.4. *Causes of the trimodal distribution*

The separation between the Aitken and accumulation modes can be explained readily by cloud processes (Hoppel et al., 1994a) in which cloud droplet nucleation on particles greater than some critical size allows them to grow rapidly via uptake of gas phase material, e.g., SO_2, followed by aqueous phase oxidation. This critical size is dependent on the particle chemistry and water vapor supersaturation in the clouds. Given that the submicrometric, Arctic MBL aerosol contained significant sulfate or other soluble compounds (Leck et al. 1996) and assuming a supersaturation of about 0.15% to 0.2% in the case of stratus in the Arctic MBL this would yield a critical size of about 80 to 100 nm (Pruppacher and Klett, 1978). This diameter range corresponds with the large size tail of the Aitken mode observed in the Arctic MBL and particles in this range of the Aitken mode (and larger) are most likely to be CCN in those air parcels with the highest supersaturation in a stratus cloud. Growth during a single or several cloud passages would be adequate to shift such a particle to the accumulation mode and make it an active CCN at lower supersaturation, thus more likely to nucleate and grow further by aqueous processes in any subsequent cloud passages. This process is not limited to the Arctic MBL itself and could have occurred in clouds any time during the air parcel's history of transport to the Arctic MBL. The fact that the Aitken and accumulation modes (and the minimum between them) are so stable with respect to diameter and standard deviation indicates that the time integrated aerosol chemistry and cloud processes by which particle growth occurs are relatively constant over the varied synoptic conditions of the cruise. The source and sink processes that determine their concentrations are obviously much more variable.

The separation between the ultrafine and Aitken modes requires some other explanation since the separation diameter of 20 to 30 nm is much less than the critical size for supersaturation in clouds in the Arctic MBL during this cruise. According to model studies, bursts of new particles formed by binary nucleation can occur leading to separate modes which subsequently grow by condensation and coagulation but retain their identity (Raes and Dingenen, 1992). This requires stable uniform conditions for periods of days, however, and does not produce the constant modal properties observed during IAOE-91. Nucleation of particles is favored in air parcels with low temperature, low existing aerosol surface area, high uv radiation, high RH and high precursor gas concentrations (Raes et al., 1993; Peters and Easter, 1994). This condition is most likely to occur in air in the outflow or detrainment regions near the tops of precipitating clouds in the MBL from which particles have been scavenged to reduce the surface area for condensation on existing particles (Hegg et al., 1990). If such nucleation occurred, then air parcels containing the resulting ultrafine mode could be mixed with adjacent air parcels within the stable boundary layer and on occasion down to the mixed layer and the surface below (see Nilsson (1996) for details of the boundary layer structure). The adjacent air parcels containing Aitken and accumulation aerosol could not support nucleation due to the higher available particulate surface area even if gas phase concentrations and other conditions were favorable for nucleation.

3.5. *Comparison of measurements of the ultrafine particle mode concentration*

The ultrafine aerosol in the range between 2.7 and 5 ± 1 nm was observed with two instruments, the UDMPS and the UCPC:PHA. The comparison of the results for some high concentration events presented by Wiedensohler et al. (1994) was good and generally within the experimental uncertainties. However, the overall comparison during the cruise was not strong due to several factors. The combined effect of particle loss and the transfer function in the UDMPS system has been determined to be larger and more uncertain that was expected. The lifetime of particles in this small and narrow size range is comparable to the one hour averaging time of the data obtained intermittently during the hour such that the timing of the measurements may not have been adequately matched. The upper limit of calibration of the UCPC:PHA is uncertain and may not match the 2.7 to 5 nm integral of the UDMPS. Instrumental errors and counting uncertainties of the UDMPS

cause an uncertainty of greater than ±50% when the hourly average concentration in this range is less than 10 cm^{-3}. For the 33 h when there was data at concentrations greater than this the regression coefficient, R^2, was 0.6. The UDMPS concentration was low by a factor of ten to twenty in the 2.7 to 5 nm range compared to the UCPC:PHA.

In consideration of this result and the result of the intercomparison before the cruise the UCPC:PHA data should be considered the better set for the size range 2.7 to 5 nm. The frequency distribution of number concentration determined by the UCPC:PHA is presented in Fig. 6 and shows that the most frequent concentrations were either less than 0.01 cm^{-3} or in the range 0.1 to 10 cm^{-3}.

Considering this UCPC:PHA data, the ultrafine mode that was observed with the UDMPS, fit with DistFit™ and represented in the frequency of occurrence plots (Figs. 4b, 5) does not apply to the particle concentration in the range less than 5 nm that represents the most recently produced particles and is the best indicator of new particle formation. On average, a mode between 10 and 20 nm geometric mean diameter dominated the particle concentration less than 25 nm diameter. However, the UCPC:PHA data show that there was a concentration greater than 0.01 cm^{-3} in the size range between 2.7 and 5 nm 52% of the time which was not generally detected by the UDMPS and thus not fit or modeled by DistFit™. According to Fig. 6 there must have been a concentration greater than 1 cm^{-3} in this subrange 32% of the time. This is greater than the concentration that can be predicted by the tail of the ultrafine mode at these sizes from the modal fit and statistics data. Thus, this data suggest the existence of a smaller, lower concentration ultrafine mode that occurs either concurrently with the 10 to 20 nm ultrafine mode or when it is absent. This result implies a lower but more continuous production rate of new particles in the Arctic MBL than that inferred from the less frequent but more concentrated ultrafine mode at 10 to 20 nm.

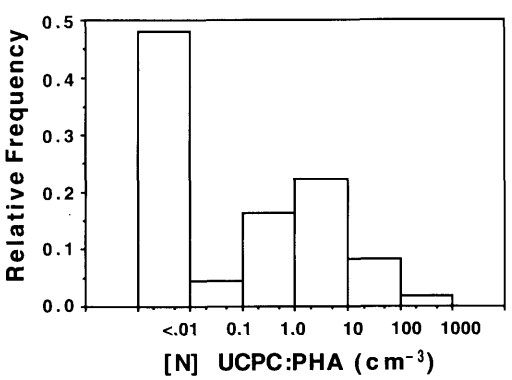

Fig. 6. Frequency of occurrence of aerosol concentration in the size range 2.7 to 5 nm determined by the UCPC:PHA during the IAOE-91 cruise.

4. Summary

General features of the aerosol in the size range 3 to 500 nm diameter in the Arctic MBL during the Summer have been quantified as a result of the IAOE-91 on the *Oden*. This is the first extensive, highly size resolved observation of aerosol over this size range in the Arctic MBL and provides a rich data set which can be applied to a number of studies including aerosol, cloud and radiative transfer modeling.

The distribution was characterized by three submicrometric modes, with geometric mean diameters of 170 nm, 45 nm and 14 nm. There were clear minima in number concentrations between the modes that appear at 20 to 30 nm and at 80 to 100 nm. The total number concentration was most frequently between 30 and 60 particles cm^{-3} with a mean value of around 100 particles cm^{-3}, but the concentration varied over two to three orders of magnitude during the 70 days of the expedition. The highest concentration was generally in the accumulation mode that contained about 45% of the total number, while the Aitken mode contained about 40%. The greatest variability was in the ultrafine mode concentration. The geometric mean diameters and the standard deviations of the modes, especially the Aitken and accumulation modes, were relatively constant independent of concentration and air mass source.

The size distributions can be accurately represented by log normal fits to the three individual modes thus reducing the data set to a time series of nine parameters of which only three, the number concentrations had much variability. The ultrafine mode mean diameter also showed some degree of variability. The other parameters were relatively constant.

The source of the Aitken and accumulation mode aerosol in the Arctic MBL in the Summer and Autumn appears to be a combination of two processes. On some, few occasions this aerosol may be present due to long range transport, largely aloft, from distant anthropogenic sources on the continents. More often it seems to be due to production and transformation from naturally occurring gas phase precursors within the Arctic region and the MBL. The new, ultrafine particles seem to be produced not generally within the overall MBL but in a layer of the MBL above the surface. The trimodal nature of the size distribution is indicative of two meteorological processes that are active in producing the observed aerosol. The separation between the Aitken and accumulation modes about 80 nm is indicative of and consistent with cloud processing by which the largest of the Aitken particles are nucleated to cloud droplets followed by heterogeneous growth to produce accumulation mode-sized particles upon evaporation. The separation between the ultrafine and Aitken mode and the sporadic nature of high concentrations in the ultrafine mode are an indication that rapid nucleation of new particles is not an active process in throughout the MBL but occurs near the top of the stable boundary layer or in the free troposphere and that parcels of air containing high concentrations of ultrafine particles are mixed into the MBL with the Aitken and accumulation modes. By contrast, the more general presence of particles in the 2.7 to 5 nm range is indicative of a lower but more continuous production rate of particles in the MBL.

5. Acknowledgments

We are grateful to the crew of the icebreaker *Oden* (chartered from the Swedish National Maritime Administration by the Swedish Polar Research Secretary) for their assistance and cooperation in making successful atmospheric sampling possible. This research was funded by the National Science Foundation, Division of Atmospheric Chemistry, (grant ATM 9008443) and the Swedish Natural Science Research Council (contract E-EG/GU 9906-303/E-EG 3922-313) and the Knut and Alice Wallenberg Foundation.

REFERENCES

Albrecht, B. A. 1989. Aerosols, cloud microphysics, and fractional cloudiness. *Science* **245**, 1227–1230.

Bigg, E. K., Leck, C. and Nilsson, E. D. 1996. Sudden changes in arctic atmospheric aerosol concentrations during summer and autumn. *Tellus* **48B**, this issue.

Charlson, R. J., Langner, J. and Rodhe, H. 1991. Perturbation of the northern hemisphere radiative balance by backscattering of anthropogenic sulfate aerosols. *Tellus* **43AB**, 152–163.

Charlson, R. J., Schwartz, S. E., Hales, J. M., Cess, R. D., Coakley, J. A., Hansen, J. E. and Hofmann, D. J. 1992. Climate forcing by anthropogenic aerosols. *Science* **256**, 423–430.

Clarke, A. D. 1993. Atmospheric nuclei in the Pacific mid-troposphere: Their nature, concentration and evolution. *J. Geophys Res.* **98D**, 20633–20647.

Covert, D. S. and Heintzenberg, J. 1993. Size distribution and chemical properties of aerosol at Ny-Ålesund, Svalbard. *Atmos. Environ.* **27A**, 2989–2997.

Covert, D. S., Kapustin, V. N., Quinn, P. K. and Bates, T. S. 1992. New particle formation in the marine boundary layer. *J. Geophys. Res.* **97**, 20581–20589.

Davidson, C. I. and Schnell, R. 1993. Arctic air and snow chemistry. *Atmos. Environ.* **27A**, 2695–2703.

Durkee, P. A., Pfeil, F., Frost, E. and Shema, R. 1991. Global analysis of aerosol particle characteristics. *Atmos. Environ.* **25A**, 2457–2471.

Easter, R. C. and Peters, L. K. 1994. Binary homogeneous nucleation: temperature and relative humidity fluctuations, non-linearity and aspects of new particle production in the atmosphere. *J. Appl. Meteor.* **33**, 775–784.

Hegg, D. A., Radke, L. F. and Hobbs, P. V. 1990. Particle production associated with marine clouds. *J. Geophys. Res.* **95**, 13917–13926.

Heintzenberg, J. and Leck, C. 1994. Seasonal variation of the atmospheric aerosol near the top of the marine boundary layer over Spitsbergen related to the Arctic sulphur cycle. *Tellus* **46B**, 52–67.

Hoppel, W. A., Frick, G. M., Fitzgerald, J. W. and Larson, R. E. 1994a. Marine boundary layer measurements of new particle formation and the effects nonprecipitating clouds have on aerosol size distribution. *J. Geophys. Res.* **99**, 14443–14459.

Hoppel, W. A., Frick, G. M., Fitzgerald, J. W. and Wattle, B. J. 1994b. A cloud chamber study of the effect that nonprecipitating water clouds have on the aerosol size distribution. *Aerosol Sci. Tech.* **20**, 1–30.

Ito, T. 1993. Size distribution of Antarctic submicron aerosols. *Tellus* **45B**, 145–159.

Junge, C. 1972. Our knowledge of the physico-chemistry of aerosols in the undisturbed marine environment. *J. Geophys. Res.* **77**, 5183–5200.

Knutson, E. O. and Whitby, K. T. 1975. Aerosol classification by electric mobility: apparatus, theory, and applications. *J. Aerosol Sci.* **6**, 443–451.

Lannefors, H., Heintzenberg, J. and Hansson, H.-C. 1983. A comprehensive study of physical and chemical parameters of the Arctic summer aerosol; results from the Swedish expedition Ymer-80. *Tellus* **35B**, 40–54.

Leck, C. and Persson, C. 1996a. The central Arctic Ocean as a source of Dimethyl Sulfide, Seasonal variability in relation to biological activity. *Tellus* **48B**, this issue.

Leck, C. and Persson, C. 1996b. Seasonal and short-term variability in dimethyl sulfide, sulfur dioxide and biogenic sulfur and sea salt aerosol particles in the arctic marine boundary layer during summer and autumn. *Tellus* **48B**, this issue.

Leck, C., Bigg, E. K., Covert, D. S., Heintzenberg, J., Maenhaut, W., Nilsson, E. D. and Wiedensohler, A. 1996. Overview of the Atmospheric research program during the International Arctic Ocean Expedition of 1991 (IAOE-91) and its scientific results. *Tellus* **48B**, this issue.

Liu, B. Y. H. and Pui, D. Y. H. 1974. A submicron aerosol standard and the primary, absolute calibration of the condensation nuclei counter. *J. Colloid and Interface Sci.* **47**, 155–171.

Nilsson, E. D. 1996. Planetary boundary layer structure and air-mass transport during the International Arctic Ocean Expedition, 1991. *Tellus* **48B**, this issue.

Nilsson, E. D. and Bigg, E. K. 1996. Influences on formation and dissipation of high arctic fogs during summer and autumn and their interaction with aerosol. *Tellus* **48B**, this issue.

Penner, J. E., Dickinson, R. E. and O'Neill, C. A. 1992. Effects of aerosol from biomass burning and the global radiation budget. *Science* **256**, 1432–1434.

Pruppacher, H. R. and Klett, J. D. 1978. *Microphysics of clouds and precipitation.* Reidel Publishing Co., Dortrecht 714 pp.

Radke, L. F., Coakley, J. A. and King, M. D. 1989. Direct and remote sensing observations of the effects of ships on clouds. *Science* **246**, 1146–1149.

Raes, F. and Van Dingenen, R. 1992. Simulations of condensation and cloud condensation nuclei from biogenic SO_2 in the remote marine boundary layer. *J. Geophys. Res.* **97**, 12901–12912.

Raes, F., Van Dingenen, R., Wilson, J. and Saltelli, A. 1993. *Cloud condensation nuclei from dimethyl sulphide in the natural marine boundary layer. Remote versus in-situ production.* Kluwer Academic Publisher, Dortrecht: 311–322.

Rahn, K. A. 1981. Atmospheric, riverine and oceanic sources of seven trace constituents to the Arctic ocean. *Atmos. Environ.* **15**, 1507–1516.

Twomey, S. 1977. *Atmospheric aerosols.* Elsevier Scientific Publishing Co., Amsterdam, 302 pp.

Whitby, E. R., McMurry, P. H., Shankar, U. and Binkowski, F. S. 1991. *Modal aerosol dynamics modeling.* U. S. Environmental Protection Agency, Atmospheric Research and Exposure Assessment Laboratory, 68-01-7365.

Wiedensohler, A. 1988. An approximation of the bipolar charge distribution for particles in the submicron size range. *J. Aerosol Sci.* **19**, 387.

Wiedensohler, A., Aalto, P., Covert, D., Heintzenberg, J. and McMurry, P. H. 1994. Intercomparison of four methods to determine size distributions of low concentration ($\sim 100\,cm^{-3}$), ultrafine aerosols ($3 < D_p < 10$ nm) with illustrative data from the Arctic. *Aerosol Sci. Technol.* **21**, 95–109.

Winklmayr, W., Reischl, G. P., Lindner, A. O. and Berner, A. 1991. A new electromobility spectrometer for the measurement of aerosol size distributions in the size range from 1 to 1000 nm. *J. Aerosol. Sci.* **22**, 289–296.